

Cellular Nanomedicine

## Distinct contributions of microtubule subtypes to cell membrane shape and stability

Andrew E. Pelling, PhD,<sup>a,b,c</sup> David W. Dawson, MD, PhD,<sup>d</sup> David M. Carreon,<sup>d</sup>  
Jason J. Christiansen, PhD,<sup>d</sup> Rhine R. Shen, PhD,<sup>d</sup>  
Michael A. Teitell, MD, PhD,<sup>c,d,e,\*</sup> James K. Gimzewski, PhD<sup>b,c,\*</sup>

<sup>a</sup>Department of Medicine and the London Centre for Nanotechnology and, University College London, London, United Kingdom

<sup>b</sup>Department of Chemistry and Biochemistry, University of California, Los Angeles, Los Angeles, CA, USA

<sup>c</sup>California NanoSystems Institute, University of California, Los Angeles, Los Angeles, CA, USA

<sup>d</sup>Department of Pathology and Laboratory Medicine, David Geffen School of Medicine, University of California, Los Angeles, Los Angeles, CA, USA

<sup>e</sup>Molecular Biology Institute and Jonsson Comprehensive Cancer Center, David Geffen School of Medicine, University of California, Los Angeles, Los Angeles, CA, USA

Received 12 September 2006; accepted 21 November 2006

### Abstract

Microtubules (MTs) are linked to cell mechanobiology. “Stable” and “dynamically unstable” microtubule (MT) subtypes are differentially sensitive to growth and distribution in serum starved (SS) versus full serum (FS) conditions. Atomic Force and Immunofluorescence microscopies were used to study the nanomechanical properties of the cell membrane in response to serum conditions and nocodazole. Nanomechanical properties of the cell membrane remain unchanged under SS/FS conditions even though there are drastic MT changes. The cell membrane is shown to depend on unstable MTs and the intermediate filament (IF) networks to maintain local stiffness. Measurements of local membrane nanomechanics in response to nocodazole display characteristic serum dependent decays. The responses suggest that the cell exists in a mechanical transition state. Stiffness is shown to depend on the interplay between dynamically unstable MTs, stable MTs and IFs which all act to impart a distinct cellular type of transient “metastability”.

© 2007 Elsevier Inc. All rights reserved.

### Key words:

Atomic force microscopy; Microtubules; Nocodazole; Metastability; Young's modulus

### Background

Microtubules (MTs) are found extensively throughout the cell in the cytoplasm between the nucleus and the cell membrane. The amount of surface area they represent inside the cell ( $\sim 1000 \mu\text{m}^2$ ) has been reported to be on par with the surface area of the plasma membrane [1]. Consequently,

MTs represent an enormous substrate for biochemical reactions taking place inside the cell [1]. They are also dynamic structures, able to grow and depolymerize in response to signaling pathways and environmental conditions [1–9]. In-vivo, MTs can exist either as “dynamically unstable” tyrosinated MTs (Tyr-MT) [2] with a turnover rate of 5–10 mins [3–8] or “stable” detyrosinated MTs (Glu-MT) [4,9] with a turnover of  $\sim 18$  hrs [3–8] (Table 1). Nature has taken advantage of the dynamics, polarity and pervasiveness of MTs by using them as major components of important signaling pathways throughout the cell.

In addition to being inextricably linked to cell biochemistry, MTs also play an important role in the mechanical properties of the cell in conjunction with actin and intermediate filaments (IFs) [10,11]. Several theoretical models describing cell mechanics have been developed in

No conflict of interest was reported by the authors of this paper.

\* Corresponding authors. James K. Gimzewski, Department of Chemistry and Biochemistry, University of California, Los Angeles, Los Angeles, CA 90095, USA. Michael A. Teitell, Department of Pathology and Laboratory Medicine, University of California, Los Angeles, Los Angeles, CA 90095-1732, USA.

E-mail addresses: [mteitell@ucla.edu](mailto:mteitell@ucla.edu) (M.A. Teitell), [gim@chem.ucla.edu](mailto:gim@chem.ucla.edu) (J.K. Gimzewski).

Table 1  
Differences in MT distributions and nocodazole susceptibility in response to serum conditions<sup>a</sup>

	Tyr-MTs		Glu-MTs	
	SS	FS	SS	FS
Present in vivo	Y	Y	N	N
Nocodazole susceptibility	Y	Y	N/A	N

Abbreviations: FS, full serum; Glu-MTs, detyrosinated microtubules; SS, serum starved; Tyr-MTs, tyrosinated microtubules.

<sup>a</sup> Data from references [2–9].

the past and each of these models takes a different approach to describing the relative roles of cytoskeletal filaments. Specifically, MTs are most commonly modeled either as one element within a cytoplasmic viscoelastic continuum [10], compression elements within a tensegrity framework [12–14], or forming part of a porous cytoskeletal network [15–18] which may act against the osmotic pressure of the cytoplasm [19]. Several experimental methods such as microrheology [20–23], atomic force microscopy (AFM) [24], micropipette aspiration and others [10] currently exist to test these models and probe the mechanical properties of cells.

The AFM has found unique applications in the measurement of the very local (<100 nm<sup>2</sup>) mechanical properties of living cells [20,21,23,25–29]. Maps of the local Young's Modulus (or elasticity,  $E$ ) of the whole cell surface can be created using AFM force-volume techniques at low resolution (~0.5–1.5  $\mu$ m) and over a period of 20–30 minutes [25–27,30,31]. However, an accepted drawback of this method in some experimental situations can be the long imaging time. Cytoskeletal dynamics occur with times much faster than 20–30 mins [3–8,32], which precludes the resulting force map from showing dynamic nanomechanical responses with high temporal resolution. However, this has not prohibited investigations of the long term effect of actin and MT depolymerizing drugs on the mechanical properties over the whole cell membrane [27]. Although the AFM is well suited to investigations of local cell mechanics it has not been used to investigate the local mechanical role of both subtypes of MTs which were discussed above. Here, mechanical properties of these distinct populations of MTs were measured by controlling their presence and distribution through varying physiological conditions. The results reveal that in NIH3T3 cells “dynamically unstable” Tyr-MTs in concert with IFs maintain cell stiffness under varying serum conditions while the presence of Glu-MTs imparts a distinct type of “metastability” in response to the MT depolymerizing drug nocodazole.

## Methods

### Cell culture

NIH3T3 cells were cultured in DMEM (Invitrogen) supplemented with 10% fetal bovine serum (HyClone), 50 U/ml penicillin, 50  $\mu$ g/ml streptomycin, 50  $\mu$ g/ml sodium

pyruvate, and 50  $\mu$ g/ml non-essential amino acids. Cells were split into SS or FS medium at low density 48 hrs prior to the start of AFM measurements. Two hrs prior to AFM studies, the cells were washed once with PBS and replaced with CO<sub>2</sub>-independent medium (Invitrogen) with or without serum. Nocodazole (methyl[5-(2-thienyl-carbonyl)-1H-benzimidazol-2-yl]-carbamate, Sigma) was prepared as a stock solution in DMSO vehicle and diluted to a final concentration of 10  $\mu$ M for AFM measurements. DMSO controls were performed with identical volumes of DMSO.

### Nanomechanical analysis with atomic force microscopy

Individual cells were chosen by optical inspection using an inverted optical microscope (Nikon Eclipse TE200) combined with an AFM (Bioscope, Veeco Digital Instruments) and a temperature controlled stage set to 37°C. The AFM tip was positioned over the nucleus of the chosen cell and brought into contact with the cell using the AFM software. The scan size was set to 0 nm to prevent scanning of the AFM tip and to maintain a constant position on the cell. Force measurements were made with soft SiN<sub>4</sub> triangular cantilevers with experimentally determined [33] spring constants of 0.02  $\pm$  0.01 N/m (Olympus Oxide Sharpened OTR4 cantilevers).

Force-displacement curves were measured at 1 Hz and were used to extract the local nanomechanical Young's modulus ( $E$ ) by fitting with the Hertz model which describes the indentation of an elastic sample with a stiff cone and is described elsewhere [26–28]. Results were analyzed in the force range of 100–300 pN, which results in shallow indentations (<200 nm) into the cell [34]. This prevented damage to the cell membrane and spurious results induced by substrate effects which can be significant with nanomechanical measurements of thin samples [26–28].

After the initial force curve was measured, 1 mL of 40  $\mu$ M Nocodazole was injected into the tissue culture dish (for a final concentration of 10  $\mu$ M) and force curves were measured once every minute for 30 mins and once every 10 mins thereafter until 1 hr had elapsed. Control experiments were performed by injecting 1 mL of nocodazole-free DMSO/media solution and force curves were collected in the same manner. All injections were warmed to 37°C before the injection to reduce the effect of thermal fluctuations.

### Flow cytometry

Cells were split directly from CO<sub>2</sub>-independent SS or FS cultures used for AFM measurements and treated with nocodazole for 0, 1, 10, 60, or 240 mins. For apoptosis analysis, 5  $\times$  10<sup>5</sup> cells were harvested and stained with FITC-conjugated-annexin V antibody and propidium iodide (BD Pharmingen, San Diego, CA) for 30 m at 25°C. Flow cytometry was performed with a FACSCalibur (BD Pharmingen). Annexin V- positive/PI-positive cells were expressed as a percentage of total cells.

## Immunofluorescence

### *Actin immunofluorescence*

Cells were fixed on the culture dishes with 3.5% formaldehyde for 10 mins, rinsed three times with PBS, and permeabilized in 0.1% Triton X-100 for 3 mins. The cells were then stained with Phalloidin-TRITC (Sigma) for 20 mins at room temperature and then rinsed with PBS three times and mounted on glass slides with vectashield (Vector Labs, Burlingame, CA). In some cases the DNA was labeled with DAPI (Invitrogen) on ice for 10 minutes prior to mounting.

### *Microtubule and intermediate filaments*

Cells were grown on 18-mm round glass cover slips in 6-well flat-bottom plates to a confluence of  $\sim 5 \times 10^4$  cells/cm<sup>2</sup>. The cells were fixed on the cover slip using cold methanol ( $-20^\circ\text{C}$ ) for 30 minutes. They were rinsed twice with PBS and then incubated with the primary antibody (anti-tyrosinated tubulin (Abcam), anti-detyrosinated tubulin (Abcam) or anti-vimentin (Sigma)), for 1 hr at  $25^\circ\text{C}$  in a humidified chamber. The cells were rinsed three times with PBS for 10 mins each. The cells were then incubated with the fluorescently labeled secondary antibody (anti-rat or anti-mouse, Sigma) for 30 mins at  $25^\circ\text{C}$  in a humidified chamber. The slides were rinsed three times with PBS for 10 mins each and mounted on glass slides with Vectashield. MTs were imaged with an Olympus AX70 upright microscope and CCD camera (UCLA). Actin and Intermediate filament images were captured with an ORCA-AG Deep Cooled CCD mounted on an IX71 Olympus inverted optical microscope (London Centre for Nanotechnology).

## Results

### *The local nanomechanical properties of the cell membrane under SS and FS conditions*

Tyr- and Glu-MTs, IFs and the actin networks were assessed in NIH3T3 fibroblasts under serum starved (SS) and full serum (FS) conditions (Figure 1). Consistent with previous studies [2-8,35], Tyr-MTs were present under both SS and FS conditions (Figure 1, A and B), while Glu-MTs were only present under FS conditions (Figure 1, C and D). Intermediate filaments (IFs) displayed a slight collapse around the nucleus under SS conditions but remained fairly spread throughout the cytoplasm as expected [11]. Notably, actin fibers were not significantly altered in appearance after serum, as expected [36] (Figure 1, E-H).

Given these dramatic differences in microtubule architecture under SS/FS conditions, one would reasonably expect that the mechanical properties of the plasma membrane [26-28] of living cells would differ significantly. In order to measure  $E$ , an AFM tip was positioned over the center of single cells using light microscopy [29]

and force curves were measured (Figure 1, I). Although not all cells were structurally identical, a large number of measurements ( $n = 65$  cells) were made to determine an average modulus in either SS or FS conditions. Force curves were fitted with a Hertzian analysis as described in detail previously [26-28]. Force curves were always measured over the highest part of the cell and with small indentations to avoid substrate effects ( $<10\%$  as defined by Bueckle's indentation depth limit [34]). Although the cell nucleus is most likely very close to the plasma membrane it has been shown extensively in the literature that this region of the cell is the softest and that the leading edges suffer most from surface effects [25-27]. Therefore although the apparent stiffness in this region is a result of several structural elements within the cell we assume the nucleus does not effect the apparent  $E$  as significantly as the substrate under a thin leading edge. Hertzian fits to the data (Figure 1, J and K) typically had correlation coefficients  $R^2 > 0.99$  indicating that the model adequately described the mechanical properties of the cell membrane under small deformations.

The average local  $E$  of the cell membrane was determined to be  $6.7 \pm 1.9$  kPa under SS conditions and  $7.0 \pm 2.3$  kPa under FS conditions (Figure 1, L and M), indicating that the local cell stiffness under SS/FS conditions is statistically indistinguishable ( $P > .4$ ). This result is surprising given that the MT architecture varied dramatically (Figure 1, A-D). The error bars in  $E$  likely reflect variability in factors such as individual cell architecture, morphology and AFM tip contact point. These results suggest that Glu-MTs, while having long turnover times, either do not contribute significantly to the structural stability of the cell or that individual cells actively maintain their shape and rigidity through an alternative mechanism possibly involving IF condensation around the nucleus (Figure 1, E and F).

### *The nanomechanical response of the cell to the MT depolymerizing drug nocodazole*

To determine the role Glu-MTs play on local cell membrane mechanics, the physical response of the cell membrane to the MT depolymerizing drug nocodazole was measured under SS conditions (Figure 2). Nocodazole preferentially targets Tyr-MTs (Figure 2, A and B), but not Glu-MTs [3,5-8] (Figure 2, C and D) or IF and actin filaments [11,37-39] (Figure 2, E-H). The lack of filamentous structures in the Tyr-MT images after 30 min of nocodazole exposure under SS/FS conditions indicates that Tyr-MTs were depolymerized. The IF network was observed to significantly condense around the nucleus after exposure to nocodazole (Figure 2, E and F) but maintained a filamentous morphology. The condensation was far less significant under FS conditions as the IFs remain further spread throughout the cytoplasm (Figure 2, F). On the other hand, the actin network did not change significantly in response to nocodazole or serum. In contrast to the AFM

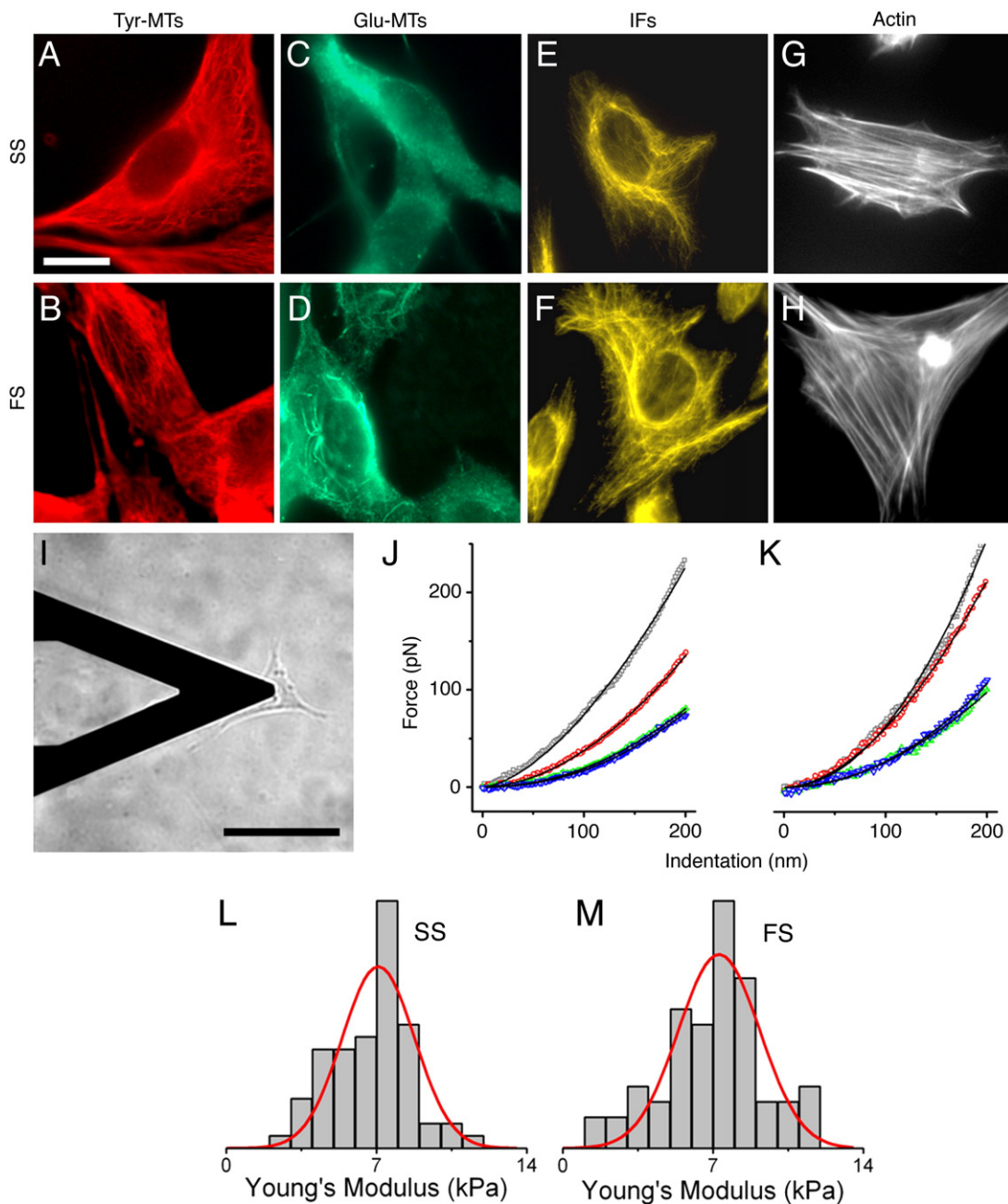


Fig 1. Serum-starvation does not alter Young's modulus in NIH3T3 cells. As visualized by immunofluorescence, tyrosinated MTs (Tyr-MTs) are present under SS/FS conditions (A, B) while dephosphorylated MTs (Glu-MTs) are only present under FS conditions (C, D) (scale bar = 20 μm and applies to a-h). The intermediate filaments (IFs) (E, F) and actin networks are clearly present under SS/FS conditions (G, H). In order to examine the local mechanical properties of cells, an AFM was used to make measurements of the cell membrane Young's Modulus (E) directly over the nucleus of the cell (I, scale bar = 100 μm). Measured force-distance curves were converted into force-indentation curves and fit with the Hertz model as described in the methods section. Force indentation curves are shown for untreated cells (grey curves) under SS (J) and FS (K) conditions. Curves are also shown for cells after exposure to nocodazole for 10 minutes (red curves), 30 minutes (green curves) and 60 minutes (blue curves) (see Figure 2, I-L). Hertzian fits are shown (black lines) and always had an  $R^2 > 0.99$  indicating that the model was capable of describing the local mechanical properties of the cell for small deformations. Normalized histograms representing the average of Young's moduli on all 65 measurements under SS (L) and FS conditions (M) show that the mechanical properties of the cell are unchanged by serum conditions.

force volume applications described above, the measurement of  $E$  in this study was localized to a single spot over the center of the cell. Although this prevents the measurement of the mechanical properties of the entire cell surface, it has the advantage of allowing a real-time examination of

the effect of nocodazole on the local mechanical properties of the cell membrane with high temporal resolution.

The  $E$  of single cells under SS conditions was determined as a function of exposure time to nocodazole over the period of one hour. We observed a ~75% decrease in  $E$  for SS cells

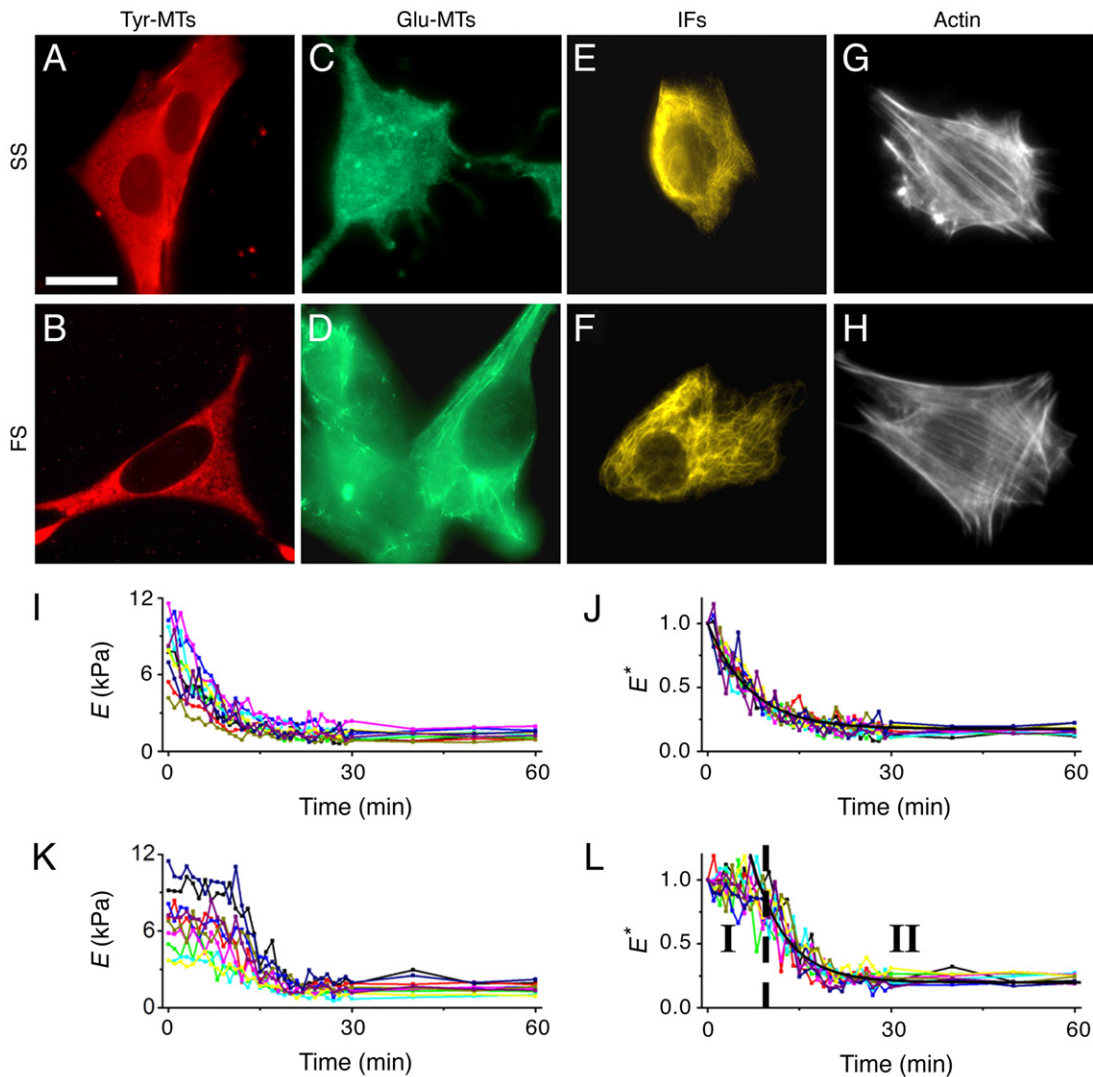


Fig 2. The kinetics of decay in plasma membrane rigidity in response to nocodazole treatment varies between SS and FS conditions. Immunofluorescence following 30 minutes of nocodazole treatment demonstrates Tyr-MTs are completely depolymerized under SS or FS conditions (A, B) (scale bar = 20  $\mu$ m and applies to A-H). In contrast, detyrosinated MTs (Glu-MTs) are not present under SS conditions to begin with (c, see also Figure 1, C) and are not susceptible to depolymerization by nocodazole under FS conditions (D). IFs are shown to condense significantly under SS conditions (E) compared with FS conditions (F). In both cases the IFs maintain a filamentous structure revealing the nocodazole does not depolymerize the network. The actin network is not affected by nocodazole under either SS or FS conditions (G, H) [40]. Using the AFM, the local Young's modulus ( $E$ ) of the cell membrane was measured before ( $t = 0$  min) and after ( $t = 1$ -60 min) the addition of nocodazole ( $n = 10$ ). Under SS conditions (I) a rapid exponential decay in the modulus is observed. In order to compensate for wide variations in the initial value of  $E_0$ , the data sets were normalized. The SS data (J) has an average time constant of  $5.7 \pm 0.4$  mins, which is consistent with the known turnover rate of Tyr-MTs. Under FS conditions (K) there is an initial ~10-20% decrease in  $E$  during the first  $9.8 \pm 1.6$  mins, followed by an exponential decay also results in an overall decrease in  $E$  by ~75%. Fitting the exponential decay after the delayed onset of the normalized FS data (L) yields an average time constant of  $4.1 \pm 1.5$  mins.

( $n = 10$ ) within the first 15 minutes of exposure, which then plateaued to a fairly constant value during the subsequent 45 minutes of observation (Figure 2, I), indicating Tyr-MT depolymerization and IF condensation play a role in determining the stiffness of the cell during nocodazole treatment as the actin network does not change significantly. For the SS cells the data in Figure 2, J were found to follow an exponential decay described by the equation  $E(t) = E_0 e^{-kt}$  (where  $t$  is the exposure time and  $k$  is the time constant which was determined to be  $k_{SS} = 5.7 \pm 0.4$  min). This exponential

equation accurately reflects the acquired data for initial values of  $E_0$  (Figure 2, J).

Nocodazole treatments were also performed under FS conditions where Glu-MTs and Tyr-MTs are present. Tyr-MTs, but not Glu-MTs, depolymerize in response to nocodazole. In contrast to nocodazole-treated SS cells, nocodazole-treated FS cells demonstrate a distinctly different decay (Figure 2, K) in cell rigidity over time ( $n = 10$ ). The data shown in Figure 2, K super-impose upon one another if their initial moduli,  $E_0$ , are normalized

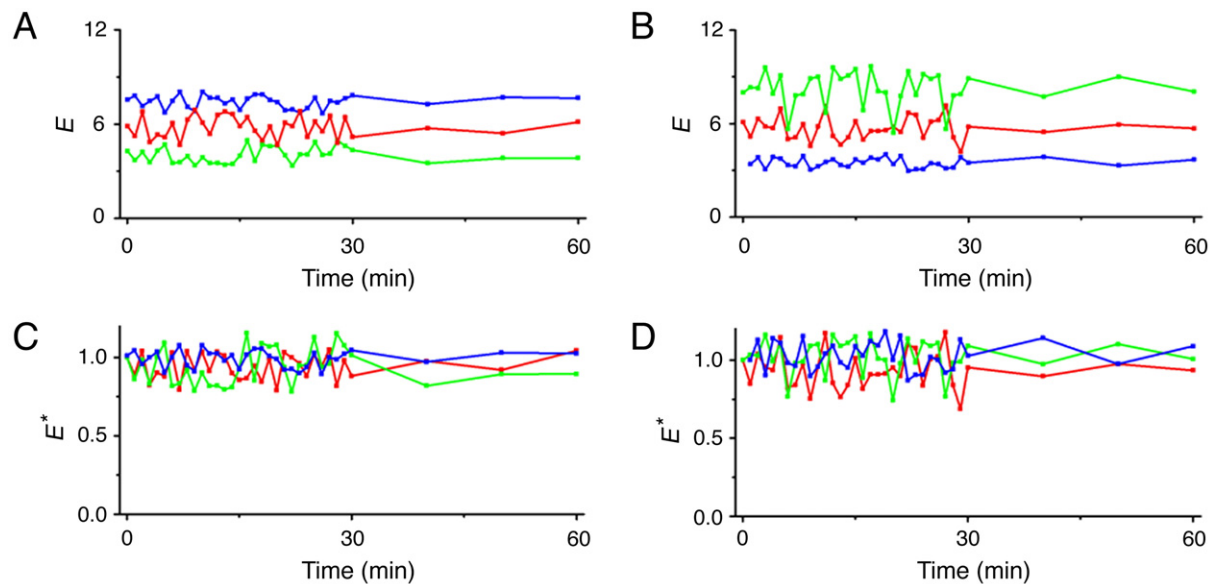


Fig 3. A series of control experiments ( $n = 3$ ) were performed in which the cells were exposed to DMSO alone in the absence nocodazole and AFM measurements were made for 60 mins. The absolute Young's Modulus is plotted for SS (A) and FS (B) conditions. The normalized modulus exhibits fluctuations over time of  $\sim 25\%$ , but it is clear that the stiffness of the cell membrane remains linear in either SS (C) or FS (D) conditions indicating that the AFM measurements are not damaging the cell membrane.

(Figure 2, L). The curves for FS nocodazole-treated cells are characterized by a slow linear decrease in  $E$  of 10–20% in the first  $9.8 \pm 1.6$  mins (I), followed by a more rapid exponential decay (II). The FS exponential decay has a  $k_{FS} = 4.1 \pm 1.5$  mins (Figure 2, J) with the notable delay in onset of  $\sim 10$  mins. Under SS conditions (Glu-MTs absent) the experimental mechanical decay in response to nocodazole treatment is a measure of the dynamics of Tyr-MT depolymerization and IF condensation kinetics, as nocodazole does not directly depolymerize actin [11,37–40]. The delayed onset of the exponential decay in rigidity as Tyr-MTs are depolymerized under FS conditions strongly suggests that the presence of Glu-MTs introduce a type of “metastability” to membrane mechanical responses.

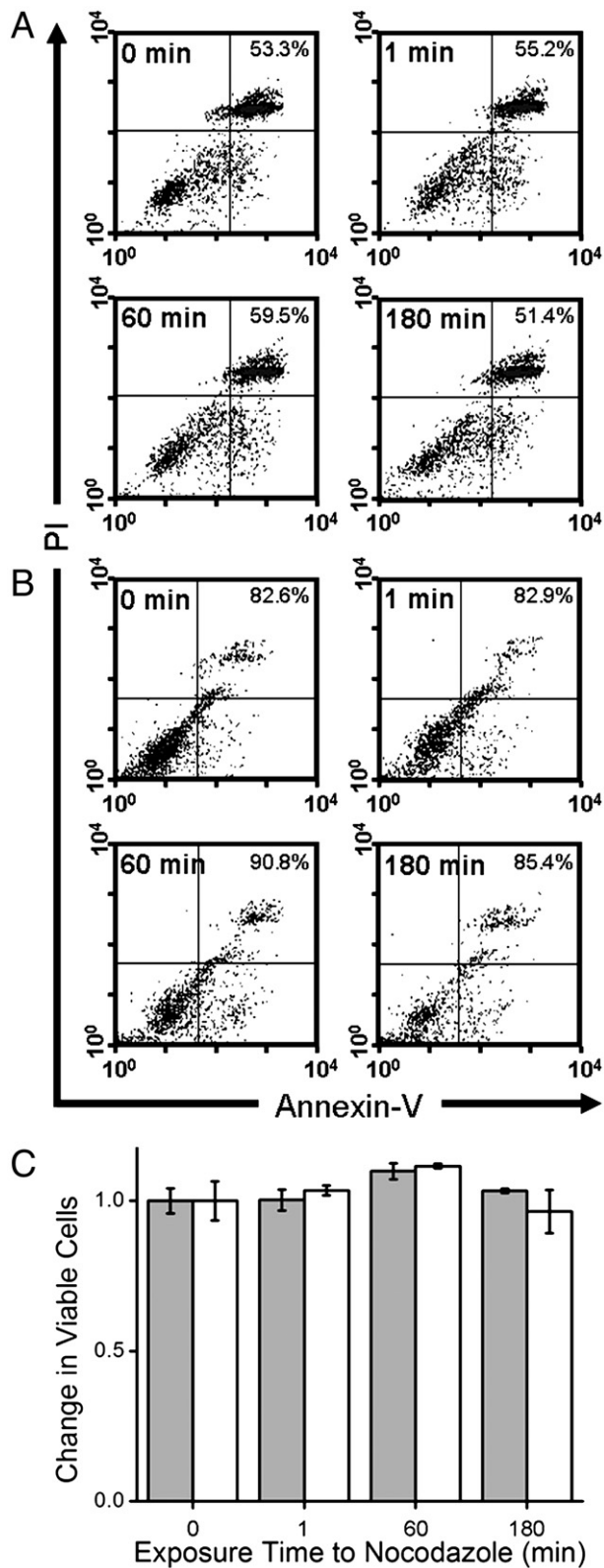
#### *The mechanical integrity of the cell membrane and cell viability under control conditions*

In previous work on different cell types it is apparent that the mechanical role of MTs on cell membrane properties can vary or display similar properties to NIH3T3 cells [27,29,41,42]. The observed decrease in  $E$  over time in our system could also arise as a consequence of experimental artifacts including: 1) damage to the cell membrane by repeated indentations by the AFM tip, 2) toxicity related to the drug vehicle (DMSO used to dissolve nocodazole) or 3) cell death resulting from apoptosis or necrosis in response to nocodazole. Excluding the first two possibilities, control AFM experiments performed with vehicle alone (DMSO without nocodazole) showed no significant mechanical differences over time under SS or FS conditions. Local fluctuations in  $E$  were observed, which may be consistent with the dynamic behavior of the cellular cytoskeleton (Figure 3). To rule out nocodazole-induced cell death flow

cytometry measurements were conducted under conditions identical to the AFM measurements. Cells were exposed to nocodazole in SS or FS conditions for up to four hours and viability was measured by flow cytometry (Figure 4, A and B). Although a higher percentage of viable cells were observed at the outset in FS compared to SS conditions (the consequence of 48 hours of serum starvation,  $\sim 83\%$  as opposed to  $\sim 53\%$  in SS), there was no significant increase in cell death or apoptosis during the period of nocodazole exposure in SS/FS conditions (Figure 4, C). Non-viable cells resulting from serum starvation typically detach or loosely adhere to the surface of a plate and therefore generally exhibit a very low stiffness or enhanced adhesion to the probe tip in AFM force measurements. Consequently, it was possible to exclude all non-viable or damaged cells at the outset by visual inspection and mechanical characterization.

#### **Discussion and conclusions**

In the first part of this study, we reported that after 48 hours of serum starvation the Tyr-MTs and actin filament networks were not significantly changed, but the Glu-MTs network was lost which has been observed previously [2,3,5–8,35,36,43]. Although the cytoskeletal network was greatly altered by the loss of Glu-MTs we did not observe any significant alteration in local cell stiffness (Figure 1, L and M). The intact IF network was observed to slightly condense around the nucleus under SS conditions and this process may allow the cell to maintain its mechanical integrity. While at first glance the results seem to suggest that Glu-MTs play no significant role in local cell membrane mechanics, under FS conditions Glu-MTs in concert with a significantly condensing IF filament network imparted a clear delayed onset in the loss



of cell stiffness due to Tyr-MT depolymerization in response to nocodazole. Importantly, the actin network was unaffected by nocodazole and serum starvation [11,36–40], indicating the important role of IFs, Glu- and Tyr-MTs in determining local cell stiffness in response to nocodazole under SS/FS conditions. Furthermore, previous work [11] has shown that stable Glu-MTs play an important role in localizing and perhaps mechanically supporting the IF network within the cell. This is consistent with our data which shows that when Glu-MTs are not present (SS conditions), IFs are found condensed around the nucleus before and more significantly after nocodazole treatment. Whereas under FS conditions the IF network appears far more spread throughout the cytoplasm, likely associated with an intact Glu-MT network [11].

Although the nanomechanical measurements during AFM were repeated on 10 cells it is important to note that in several cases cells were observed to migrate away from the tip during force curve measurements. Likewise, nocodazole treatment also resulted in many cells undergoing complete rounding causing force curves to become unusable. In these cases, the experiment was stopped and a new sample was used. However, an important observation was made during immunofluorescence imaging which may suggest that cellular responses to nocodazole may not be completely uniform. Under FS conditions it was noted that three significant populations of cells existed after nocodazole treatment in approximately equal proportions (Figure 5, A). In response to nocodazole cells either remained spread, slightly shrunken or completely rounded. In all cases except complete rounding the cells maintained an intact actin filament system. The difference between the well spread and slightly shrunken cells may account for the large variability we observed in absolute modulus values. Similar results were identified under SS conditions (data not shown), however under SS conditions only a small percentage of cells remained large and spread while the majority cells did appear to under go some shrinkage or complete rounding. In all cases, the nuclei (Figure 5, B) of cells were not observed to be significantly altered by nocodazole and completely rounded cells did not display any intact actin filaments. These results suggest that the nanomechanical dynamics we report here in response to nocodazole treatment are not uniform across an entire cell population.

Therefore, we propose that in the majority (one half to two thirds) of NIH3T3 cells in a given population, the presence of Glu-MTs in addition to an intact IF network

Fig 4. Changes in membrane properties are not the consequence of cell death or drug toxicity. Flow cytometry was also performed to ensure that the conditions of study do not induce changes in cell death, apoptosis, or necrosis during the course of analysis, especially during the initial AFM data acquisition period. Initial populations of viable cells remain constant after 1 min, 1 hr and 3 hrs of exposure to nocodazole under SS (A) and FS (B) conditions (the viable population of cells is listed as percentages in the top right hand corner of each plot). Although the absolute number of viable cells is different under SS and FS conditions, the population of viable cells does not change during exposure to nocodazole (C).

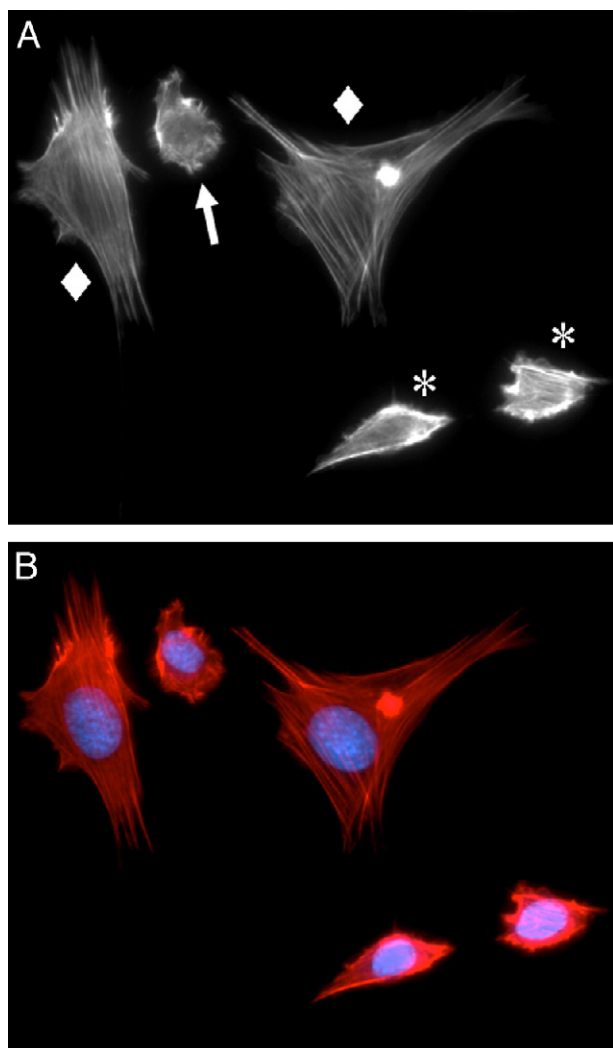


Fig 5. A distribution of cell shape and actin morphologies occur in populations of cells exposed to nocodazole. A lower magnification image (A) of the cell shown in Figure 1, H reveals that cells under FS conditions and exposed to nocodazole for 30 minutes will either remain spread while maintaining stable actin filaments (◆), slightly shrink and continue to display stable actin filaments (\*) or round up completely and display little or no filamentous actin structure (arrow). The population of each type of cell response was equally distributed under FS conditions. Under SS conditions cells either displayed a small amount of shrinking similar to those shown here or round up (data not shown). During AFM experiments round cells were never included in the analysis because force curves became very difficult to acquire due to the softness of the cell and their loose adherence to the substrate. Under all conditions the nuclei (B) of cells exposed to nocodazole never displayed any significant morphological changes (actin – red, nuclei – blue).

appears to provide a form of “metastability” important for local plasma membrane mechanical properties. After 48 hrs of serum starvation the cells appear able to dynamically adapt to maintain their local mechanical stiffness in spite of the absence of Glu-MTs and this may be achieved through unstable Tyr-MT re-organization and IF condensation around the nucleus. Furthermore, Glu-MTs appear to maintain the local mechanical stiffness of the cell in the

presence of nocodazole until some critical mass of Tyr-MTs has been depolymerized. In agreement with previous literature [11], immunofluorescence imaging suggests that the presence of Glu-MTs supports the IF network which helps to establish the delayed onset in Young’s modulus decay. This important observation reveals that the metastability imparted by Glu-MTs is highly dependent on physiological conditions and the internal biochemistry of the cell. The ability to compensate for cell stiffness with such a significant alteration in cytoskeletal integrity is clearly an important adaptive property, allowing a cell to maintain its essential structural and metabolic functionality. This adaptability also has important implications for biological processes such as metastasis or therapies targeting the cytoskeleton in cancer. However it is clear that although MTs play an important role in cell mechanics [10,41,42], they are also linked to many important signaling pathways [1] which in turn may affect the local mechanical properties of the plasma membrane. Our results demonstrate that the cytoskeleton is not an isolated mechanical entity and its relationship to cell signaling pathways and the local plasma membrane properties is complex.

The results presented here require SS/FS conditions and are only partially consistent with the existing theories of cell mechanics including viscoelastic continuum models [10], tensegrity [12–14] and the semi-flexible polymer gel model [15–18]. These models, which either view cell mechanics as a combination of discrete elements (actin, MTs, cytoplasm) clearly do not account for two distinct populations of MTs with different mechanical properties. Our observation of intact stable actin filaments after the complete depolymerization of Tyr-MTs is also inconsistent with the tensegrity model [12–14]. Furthermore, as shown in Figure 2, I–L, it is clear that the mechanical properties of a cell are not static properties but are dynamic and responsive to environmental conditions. Therefore, mechanical models of a cell must include a dependence on time and physiological conditions.

In a physiological environment, the data shown here are consistent with an active control mechanism within the cell that balances and influences cell stiffness. The results presented here lend support to the emerging view that the cell may exist in a metastable mechanical transition state where environmental conditions and the cell type dictate the most desirable or pressure-selected mechanical pathway(s) [20,21]. Therefore, time dependent mechanical models which allow for mechanical dynamics and responses of the cell are required for advanced predicative modeling of the cell in a fluctuating physiological environment. In this case, the applicability of any particular static model in part or in whole largely depends on the adaptability of the cell type examined and the in-vitro (or in-vivo) conditions which dictate the essential mechanical dynamics and stability of the cell.

#### Acknowledgments

Partially supported by the Institute for Cell Mimetic Space Exploration - CMISE (a NASA URETI Institute

NCC 2-1364) and NIH grants CA90571, CA107300, T32CA09056, T32AI07126, and by the Margaret E. Early Medical Research Trust. M.A.T. is a Scholar of the Leukemia and Lymphoma Society. A.E.P. wishes to thank the Interdisciplinary Research Collaboration in Nanotechnology (University of Cambridge) for financial support through a generous Exploratory Grant, a portion of which enabled Intermediate Filament and Actin staining/imaging to occur at the London Centre for Nanotechnology, University College London. A.E.P. also wishes to thank Professor Michael A. Horton for helpful discussions (London Centre for Nanotechnology, University College London). The authors gratefully acknowledge Sarah E. Cross for her assistance with data processing.

## References

- [1] Gundersen GG, Cook TA. Microtubules and signal transduction. *Curr Opin Cell Biol* 1999;11:81–94.
- [2] Mitchison T, Kirschner M. Dynamic instability of microtubule growth. *Nature* 1984;312:237–42.
- [3] Gundersen GG, Kim I, Chapin CJ. Induction of stable microtubules in 3T3 fibroblasts by TGF-beta and serum. *J Cell Sci* 1994;107:645–59.
- [4] Webster DR, Gundersen GG, Bulinski JC, Borisy GG. Differential turnover of tyrosinated and detyrosinated microtubules. *Proc Natl Acad Sci U S A* 1987;84:9040–4.
- [5] Cook TA, Nagasaki T, Gundersen GG. Rho guanosine triphosphatase mediates the selective stabilization of microtubules induced by lysophosphatidic acid. *J Cell Biol* 1998;141:175–85.
- [6] Palazzo AF, Cook TA, Alberts AS, Gundersen GG. mDia mediates Rho-regulated formation and orientation of stable microtubules. *Nat Cell Biol* 2001;3:723–9.
- [7] Palazzo A, Ackerman B, Gundersen GG. Cell biology: tubulin acetylation and cell motility. *Nature* 2003;421:230.
- [8] Gurland G, Gundersen GG. Protein phosphatase inhibitors induce the selective breakdown of stable microtubules in fibroblasts and epithelial cells. *Proc Natl Acad Sci U S A* 1993;90:8827–31.
- [9] Kreis TE. Microtubules containing detyrosinated tubulin are less dynamic. *EMBO J* 1987;6:2597–606.
- [10] Zhu C, Bao G, Wang N. Cell mechanics: mechanical response, cell adhesion, and molecular deformation. *Annu Rev Biomed Eng* 2000;2:189–226.
- [11] Gurland G, Gundersen GG. Stable, detyrosinated microtubules function to localize vimentin intermediate filaments in fibroblasts. *J Cell Biol* 1995;131:1275–90.
- [12] Ingber DE, Tensegrity I. Cell structure and hierarchical systems biology. *J Cell Sci* 2003;116:1157–73.
- [13] Ingber DE, Tensegrity II. How structural networks influence cellular information processing networks. *J Cell Sci* 2003;116:1397–408.
- [14] Ingber DE. Cellular tensegrity: defining new rules of biological design that govern the cytoskeleton. *J Cell Sci* 1993;104:613–27.
- [15] Head DA, Levine AJ, MacKintosh EC. Deformation of cross-linked semiflexible polymer networks. *Phys Rev Lett* 2003;91:108102.
- [16] Head DA, Levine AJ, MacKintosh FC. Distinct regimes of elastic response and deformation modes of cross-linked cytoskeletal and semiflexible polymer networks. *Phys Rev E* 2003;68:061907.
- [17] Levine AJ, Head DA, MacKintosh FC. The deformation field in semiflexible networks. *J Phys Condens Mat* 2004;16:S2079–88.
- [18] Storm C, Pastore JJ, MacKintosh FC, Lubensky TC, Janmey PA. Nonlinear elasticity in biological gels. *Nature* 2005;435:191–4.
- [19] Charras GT, Yarrow JC, Horton MA, Mahadevan L, Mitchison TJ. Non-equilibration of hydrostatic pressure in blebbing cells. *Nature* 2005;435:365–9.
- [20] Alcaraz J, Buscemi L, Grabulosa M, Trepat X, Fabry B, Farre R, et al. Microrheology of human lung epithelial cells measured by atomic force microscopy. *Biophys J* 2003;84:2071–9.
- [21] Smith BA, Tolloczko B, Martin JG, Grutter P. Probing the viscoelastic behavior of cultured airway smooth muscle cells with atomic force microscopy: stiffening induced by contractile agonist. *Biophys J* 2005;88:2994–3007.
- [22] Tseng Y, Kole TP, Wirtz D. Micromechanical mapping of live cells by multiple-particle-tracking microrheology. *Biophys J* 2002;83:3162–76.
- [23] Mahaffy RE, Park S, Gerde E, Käs J, Shih CK. Quantitative analysis of the viscoelastic properties of thin regions of fibroblasts using atomic force microscopy. *Biophys J* 2004;86:1777–93.
- [24] Binnig G, Quate CF, Gerber C. Atomic force microscope. *Phys Rev Lett* 1986;56:930–3.
- [25] Rotsch C, Braet F, Wisse E, Radmacher M. AFM imaging and elasticity measurements on living rat liver macrophages. *Cell Biol Int* 1997;21:685–96.
- [26] Rotsch C, Jacobson K, Radmacher M. Dimensional and mechanical dynamics of active and stable edges in motile fibroblasts investigated by using atomic force microscopy. *Proc Natl Acad Sci U S A* 1999;96:921–6.
- [27] Rotsch C, Radmacher M. Drug-induced changes of cytoskeletal structure and mechanics in fibroblasts: an atomic force microscopy study. *Biophys J* 2000;78:520–35.
- [28] Matzke R, Jacobson K, Radmacher M. Direct, high-resolution measurement of furrow stiffening during division of adherent cells. *Nat Cell Biol* 2001;3:607–10.
- [29] Wu HW, Kuhn T, Moy VT. Mechanical properties of 1929 cells measured by atomic force microscopy: effects of anticytoskeletal drugs and membrane crosslinking. *Scanning* 1998;20:389–97.
- [30] Haga H, Sasaki S, Kawabata K, Ito E, Ushiki T, Sambongi T. Elasticity mapping of living fibroblasts by AFM and immunofluorescence observation of the cytoskeleton. *Ultramicroscopy* 2000;82:253–8.
- [31] Hofmann UG, Rotsch C, Parak WJ, Radmacher M. Investigating the cytoskeleton of chicken cardiocytes with the atomic force microscope. *J Struct Biol* 1997;119:84–91.
- [32] McGrath JL, Tardy Y, Dewey CF, Meister JJ, Hartwig JH. Simultaneous measurements of actin filament turnover, filament fraction, and monomer diffusion in endothelial cells. *Biophys J* 1998;75:2070–8.
- [33] Levy R, Maaloum M. Measuring the spring constant of atomic force microscope cantilevers: thermal fluctuations and other methods. *Nanotechnology* 2002;13:33–7.
- [34] Stolz M, Raiteri R, Daniels AU, VanLandingham MR, Baschong W, Aebi U. Dynamic elastic modulus of porcine articular cartilage determined at two different levels of tissue organization by indentation-type atomic force microscopy. *Biophys J* 2004;86:3269–83.
- [35] Gundersen GG, Kalnoski MH, Bulinski JC. Distinct populations of microtubules: tyrosinated and nontyrosinated alpha tubulin are distributed differently in vivo. *Cell* 1984;38:779–89.
- [36] Ridley AJ, Hall A. The small GTP-binding protein rho regulates the assembly of focal adhesions and actin stress fibers in response to growth factors. *Cell* 1992;70:389–99.
- [37] Zegers MM, Zaal KJ, van ISC, Klappe K, Hoekstra D. Actin filaments and microtubules are involved in different membrane traffic pathways that transport sphingolipids to the apical surface of polarized HepG2 cells. *Mol Biol Cell* 1998;9:1939–49.
- [38] Pedrosa R, Gomes P, Hopfer U, Jose PA, Soares-da-Silva P. G(i)alpha 3 protein-coupled dopamine D-3 receptor-mediated inhibition of renal NHE3 activity in SHR proximal tubular cells is a PLC-PKC-mediated event. *Am J Physiol Renal Physiol* 2004;287:F1059–66.

- [39] Chen C, Weisz OA, Stolz DB, Watkins SC, Montelaro RC. Differential effects of actin cytoskeleton dynamics on equine infectious anemia virus particle production. *J Virol* 2004;78: 882-91.
- [40] Krendel M, Gloushankova NA, Bonder EM, Feder HH, Vasiliev JM, Gelfand IM. Myosin-dependent contractile activity of the actin cytoskeleton modulates the spatial organization of cell-cell contacts in cultured epitheliocytes. *Proc Natl Acad Sci U S A* 1999;96: 9666-70.
- [41] Wang N. Mechanical interactions among cytoskeletal filaments. *Hypertension* 1998;32:162-5.
- [42] Kasas S, Wang X, Hirling H, Marsault R, Huni B, Yersin A, et al. Superficial and deep changes of cellular mechanical properties following cytoskeleton disassembly. *Cell Motil Cytoskeleton* 2005; 62:124-32.
- [43] Wehland J, Weber K. Turnover of the carboxy-terminal tyrosine of alpha-tubulin and means of reaching elevated levels of detyrosination in living cells. *J Cell Sci* 1987;88:185-203.